ACS OMEGA

http://pubs.acs.org/journal/acsodf

Article

A Comparison of Nitrate Release from Zn/Al-, Mg/Al-, and Mg−Zn/Al Layered Double Hydroxides and Composite Beads: Utilization as Slow-Release Fertilizers

Abhinandan Singha Roy, Sreejarani Kesavan Pillai, and Suprakas Sinha Ray*

Cite This: *ACS Omega* 2023, 8, 8427−8440

Read Online

ACCESS | Metrics & More | Article Recommendations

ABSTRACT: Nitrate-loaded Zn/Al, Mg/Al, and Mg−Zn/Al layered double hydroxides (LDHs) were synthesized using the coprecipitation method. The slow-release properties of LDHs were measured in powder form at various pH conditions. Sodium alginate was used to encapsulate Mg/Al LDH to produce composite beads (LB) to further slow down the release of nitrate ions. The prepared LDH samples and LB were characterized by X-ray diffraction, attenuated total reflectance Fourier transform infrared spectroscopy, thermogravimetric analysis, and inductively coupled plasma optical emission spectroscopy. The surface morphologies of LDHs and LB were obtained from scanning electron microscopy analysis. The slow-release properties of the materials were evaluated using a kinetic study of nitrate release in tap water, soil solution, as well as plant growth experiments using coriander (*Coriandrum sativum*). The nitrate release ability of LDHs and LB was compared with a soluble nitrate source. The plant growth experiments showed that all three LDHs were able to supply an adequate amount of nitrate to the plant similar to the soluble fertilizer while maintaining the availability of nitrate over extended periods. The ability of LDHs to increase soil pH was also demonstrated.

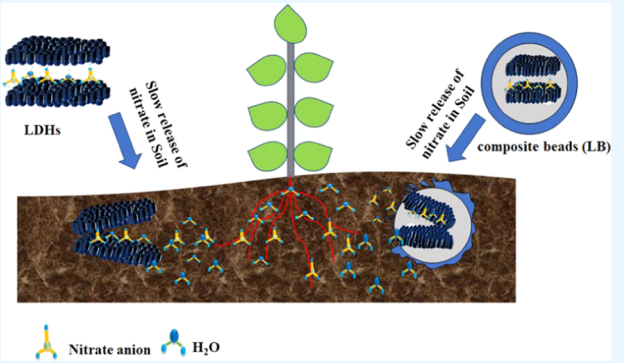

1. INTRODUCTION

For growing crops, nitrogen is generally the crucial nutrient in natural systems, and the plant uptakes nitrogen in the nitrate form. In arid and semiarid conditions, the anion-exchange capacity (AEC) of the soil is dependent on soil pH and most often is low. Soil particles may not readily absorb nitrate anions; hence, the unutilized nitrate anions can easily leach to the deeper soil layers, which is a major cause of serious surface/groundwater contamination as well as environmental pollution.[1,2] Various methods such as crop rotation, using nitrification inhibitors, soil tests, and plant monitoring to prevent nitrate loss and increase crop production, have been routinely investigated in the past.[3,4] However, preventing nitrate loss through leaching and surface runoff from the agricultural field is very challenging as the nitrate ions are highly mobile in soil solution. The amount of degradation of organic nitrogenous compounds by nitrogen mineralization also plays a crucial role in nitrate leaching. To address the excessive nitrate leaching, reducing the amount of fertilizer is advocated from seedling to different crop growth stages.[1] However, the benefits in such a scenario rely on various other factors like crop classes, time of sowing, and the root system's ability to go deep into the soil horizons.[3,5]

The slow-release fertilizers, which supply a required nutrient for a prolonged period in a relatively lower quantity, are envisaged as a solution to the excessive leaching of nitrate and associated problems. However, the climatic conditions and soil profiles can profoundly affect the efficiency of the materials.[6] Slow-release fertilizers are often conventional fertilizers coated with polymeric compounds to manipulate their release characteristics. However, the use of synthetic polymers, such as resins and petroleum-based thermoplastics as coating materials, has been facing challenges and legal restrictions in terms of their limited degradation.[7] Ecologically friendly, easily available, and cost-effective solutions are therefore required to solve problems related to the currently available slow-release fertilizer technologies.

The usage of synthetic clay minerals, namely, layered double hydroxides (LDHs) in agriculture, is not extensively reported due to the abundance and focus on natural clay minerals.

Received: November 18, 2022
Accepted: January 30, 2023
Published: February 22, 2023

However, in recent years, a lot of attention has been given to developing LDH-based agro-products considering the multifunctionality of the material.[8] LDHs are derived from the structure of the mineral brucite, $Mg(OH)_2$; unlike the brucite structure, some of the divalent metal ions are replaced with trivalent metal ions in the LDH structure. LDH is with chemical formula $[M_{1-x}^{2+}M_x^{3+}(OH_2)]^{x+}(A^{n-})_{x/n}\cdot yH_2O$ [where M^{2+} is the divalent metal ions (e.g., Mg^{2+}, Zn^{2+}, Mn^{2+}); M^{3+} is the trivalent metal ions (e.g., Al^{3+}, Fe^{3+}, Cr^{3+}); A^{n-} is the intercalated anions (e.g., NO_3^-, CO_3^{2-}, Cl^-); and x is the fractional aluminum substitution in the layers, which is the metal ratio $M^{3+}/(M^{2+} + M^{3+})$]. The value of x varies preferably between 0.2 and 0.33 with the corresponding proportion of M^{2+}/M^{3+} within 2:1−4:1.[8] The ratio of M^{3+} and M^{2+} influences the anion-exchange capacity of LDH, which could range within 200−450 $cmol_c$/kg for obtaining a relatively stable LDH structure.[9] LDHs, due to their specific intercalation chemistry and high anion-exchange capacity, can quickly release nutrient ions from the external surfaces, which is then followed by the release of intercalated nutrient ions relatively at a slower rate.[10,11] Although several methods have been employed to synthesize various binary and ternary LDHs, coprecipitation using inorganic salts is a universally employed process due to its simplicity. Many articles can be found in the literature that provides details of coprecipitation methods, which have also been used for the synthesis of LDHs[12−14] and other materials.[15−17]

According to Benício et al.,[18] LDHs can enhance the nutrient availability in the soil solution by increasing the soil pH, which increases the negative charge on the soil matrix and decreases the adsorption of anions. A recent study by Mitter et al.[19] concluded that LDH degradation occurs gradually under atmospheric CO_2 and moisture, which makes them environmentally friendly materials. Other unique characteristics of LDHs, such as high chemical stability, basicity, pH-dependent solubility, and high anion-exchange capacity, also make them prospective nanoscale agrochemicals for soil remediation, soil conditioning, as well as crop production.[8] On top of these benefits, LDHs after soil degradation can serve as a source of additional nutritional elements for plants. Hatami et al.[20] observed an increased availability of zinc in the soil after the application of phosphate-modified Zn/Al LDH. López-Rayo et al.[21] also reported an increased zinc uptake by plants on the application of Zn-doped Mg/Al LDH materials to plants. Although a variety of LDHs have been used in simulated aqueous solution environments as a nitrate ion adsorber, research reports about the capability of LDHs as slow-release nitrate fertilizers in soil conditions are scarce.[22−24] Torres-Dorante et al.[2] prepared Mg/Al LDH, which could prevent the nitrate leaching loss of up to 80% under crop conditions. Halajnia et al.[25] used Mg/Al and Mg/Fe LDH for nitrate removal from the soil solution. They reported that adsorbents did not perform efficiently for nitrate removal and noticed a decrease in nitrate adsorption at higher soil solution temperatures. Berber et al.[26] used nitrate-loaded Mg/Al LDH to release nitrate into the soil and found that the LDH was releasing nitrate slowly. Halajnia et al.[27] in another study observed that the rate of ion exchange by Mg/Al LDH depends on the soil pH; the release rate increases at lower pH due to the partial dissolution of LDH layer structures. Another observation by de Castro et al.[28] demonstrate that the structural stability rapidly decreased when the LDH was applied in a powder form in the acidic soil, affecting the slow-release behavior. Hence, to maintain the slow-release properties specifically in acidic soil conditions, encapsulation of LDH can be a good strategy.[29] Natural polysaccharides such as alginate can be a perfect option as an encapsulation matrix because of their cost-effective and eco-friendly nature.[30,31] The composite materials of LDH with such polymer systems are mutually beneficial as LDHs can contribute to the poor mechanical properties, while polymers effectively act as a barrier preventing direct contact of LDHs with acidic soil while improving the slow-release properties. Wang et al.[31] prepared biochar-impregnated calcium alginate beads with improved water holding and nutrient retention properties for soil conditioning and nutrient conservation. Karthikeyan and co-workers developed Zn/Fe LDH-encapsulated sodium alginate-functionalized beads for phosphor and nitrate ion adsorption from the aqueous environment.[32] In a recent article, Vu et al.[33] reported the synthesis of Mg/Al LDH with intercalated chloride anion and further encapsulation in sodium alginate beads for nitrate adsorption in both synthetic solution and groundwater. According to the authors, the presence of competing anions in the groundwater affected the nitrate adsorption capacity of the LDHs and its subsequent use as a slow-release nitrate fertilizer.

LDHs are progressively explored as materials to improve crop yield, quality, and soil recently. In the last few years, a few studies have been reported about the use of LDHs as slow-release fertilizers of macronutrients, such as nitrate and phosphate. These reports corroborate the studies by Everaert et al.,[10] Benício et al.,[18] and Berber et al.[26] on LDHs as promising opportunities as nanofertilizers. However, many of these studies were limited to laboratory investigations of synthesis, characterization, and release kinetics of nutrients in an aqueous or buffered solution using a single LDH material where the conclusions were drawn on experiments under controlled conditions. The data on the efficacy of different LDH materials in field trials for a specific crop in terms of nutrient bioavailability to the plant system and availability in soil is scarce.

The present work proposes a structural comparison of binary-, ternary-, and biopolymer-encapsulated LDHs along with the analysis of the performance efficacy of the materials as multifunctional slow-release nitrate fertilizers under aqueous, soil, and crop conditions. To the best of our knowledge, the present study is the first to evaluate the effect of different LDHs on nitrogen usage efficiency on the growth of coriander (*Coriandrum sativum*) in terms of soil conditioning and bioavailability to the plant, which is envisaged to add valuable knowledge to the interaction between LDHs and plants.

Hence, we herein report the synthesis of binary (Zn/Al and Mg/Al) and ternary (Mg-Zn/Al) LDHs for the intercalation and release of nitrate ions. Composite beads were prepared by encapsulating selected LDH in an alginate matrix to further slow down the nitrate release rate and induce water retention properties. The prepared materials were characterized by various instrumental techniques; nitrate release characteristics were compared and subsequently used for plant growth experiments using coriander (*C. sativum*) to evaluate the performance.

2. EXPERIMENTAL SECTION

2.1. Materials. Magnesium nitrate hexahydrate ($Mg(NO_3)_2\cdot 6H_2O$, 98%), zinc nitrate hexahydrate ($Zn(NO_3)_2\cdot 6H_2O$, 98%), aluminum nitrate nonahydrate ($Al(NO_3)_3\cdot 9H_2O$,

https://doi.org/10.1021/acsomega.2c07395
ACS Omega 2023, 8, 8427−8440

98%), hydrochloric acid (HCl), calcium sulfate ($CaSO_4 \cdot 2H_2O$), and potassium nitrate (KNO_3) were obtained from Sigma-Aldrich (South Africa). Sodium hydroxide (NaOH), acetic acid (CH_3COOH), calcium nitrate ($Ca(NO_3)_2 \cdot 6H_2O$), and sodium nitrate ($NaNO_3$) were obtained from Minema Chemicals (South Africa). Sodium alginate was obtained from SRL (Sisco Research Laboratories, India). Ultrapure water obtained by a Milli-Q system (Merck Millipore, Merck, South Africa) was used in all experimental methods.

2.2. Synthesis of LDHs. The nitrate-intercalated Mg/Al LDH was synthesized by coprecipitation with low supersaturation. Appropriate amounts of $Mg(NO_3)_2 \cdot 6H_2O$ and $Al(NO_3)_3 \cdot 9H_2O$ were weighed (using a 2:1 molar ratio) and dissolved with hot decarbonated water (100 mL) placed in a dropping funnel added dropwise with constant magnetic stirring to a 500 mL beaker containing 100 mL of 1.0 mol/L sodium nitrate solution under a N_2 gas atmosphere. Throughout the synthesis, the pH of the suspension was kept constant between 9 and 10 by adding appropriate amounts of 1.0 mol/L of NaOH dropwise into the mixture after which the white suspension was allowed to age for 18 h at 25 °C in a closed round-bottom flask. The precipitate was then washed several times with ultrapure water and dried under vacuum at 60 °C. The Mg/Al LDHs were ground, sieved to 75 μm, and kept in a closed container for further analyses and experiments. The Zn/Al and Mg−Zn/Al LDH of 2:1 ratio were synthesized using the same method. Table 1 displays the molar ratios of different precursor ions used for the synthesis.

Table 1. Molar Ratios of Different Precursor Ions Used to Synthesize Various LDHs

molar ratio (a/b/c)	Mg^{2+} (a)	Zn^{2+} (b)	Al^{3+} (c)
2:0:1	0.03	NA	0.015
0:2:1	NA	0.03	0.015
1:1:1	0.015	0.015	0.015

2.3. Synthesis of LDH-Encapsulated Beads (LB). In a typical procedure, 0.2 g of sodium alginate was mixed with 30 mL of ultrapure water in a 100 mL beaker with constant magnetic stirring. One gram of the prepared Mg/Al LDH was added to the solution and mixed for 2 h at 25 °C. The solution was subsequently added dropwise to a 250 mL beaker containing 100 mL of 0.3 mol/L $Ca(NO_3)_2 \cdot 6H_2O$ to produce hydrogel beads (LB). The prepared beads were stirred for 10 min, filtered, washed with ultrapure water, and then dried in a freeze dryer for 24 h.

2.4. Characterization. *2.4.1. LDH and LB Characterizations.* X-ray diffraction (XRD) spectra of the various LDHs (Mg/Al, Zn/Al, Mg−Zn/Al LDH), LB, and sodium alginate (SA) were obtained by an X-ray diffractometer (PANalytical X'Pert Pro, Netherlands) using Cu Kα radiation (λ =1.5406 Å) with a filament intensity of 40 mA and a voltage of 45 kV. Scans were conducted between 2θ = 1 and 40° at a scan speed of 2°/min and a scanning step of 0.02°. Infrared spectra were acquired on an attenuated total reflectance Fourier transform infrared (ATR-FTIR) spectrometer (Perkin Elmer Spectrum 100 FTIR spectrometer, USA) from 4000 to 500 cm^{-1} through eight scans at a 4 cm^{-1} resolution. A thermogravimetric analyzer (TGA) (TA Instruments TGA5500 Discovery series, USA) was used at a heating rate of 10 °C/min to study the thermal decomposition patterns of various LDHs. The surface morphology of the various LDHs was attained by a scanning electron microscope (SEM) (JEOL JSM-7500F Field Emission Electron Microscope, Japan) with an accelerating voltage of 3.0 kV and an emission current of 10 μA. To quantify the elemental components, 0.10 g of the samples was dissolved in 50 mL of 0.1 mol/L HCl solution and was diluted to a 10 ppm concentration. The amounts of Mg, Zn, and Al were determined by inductively coupled plasma optical emission spectroscopy (Perkin Elmer ICP Optima 2000 DV, USA). The amount of nitrate in LDHs was determined by ion chromatography (IC) (Dionex ICS-5000+ SP, Thermo Scientific, USA).

The anion-exchange capacity (AEC) of the prepared materials (Mg/Al, Zn/Al, Mg−Zn/Al LDH) was determined using chloride as an exchangeable anion. In a typical procedure, 500 mg of LDH was placed in 50 mL of 0.8 mol/L KCl solution in a 100 mL reagent bottle and was shaken for 24 h, and then the AEC was determined as per the procedure reported by Ito, M.[34]

2.4.2. Soil Characterization. The soil used in this study for the plant growth experiments was collected from the surface layer (0−20 cm) in the eastern region of Pretoria, South Africa. The soil was air-dried and sieved to 2 mm size to determine the physicochemical properties. The soil was characterized as follows: a hydrometer method was used to determine the percentage of sand, silt, and clay.[35] The soil sample pH was measured on 2.5:1 soil/water suspension.[36] The CEC of the soil sample was determined by the previously reported silver thiourea method.[37] Soil moisture was determined as per the method described by Okalebo et al.[36] The soil's organic matter was determined by the Walkley−Black method as per the procedure described by Schulte.[38] To determine the available nitrate in the soil, $CaSO_4 \cdot 2H_2O$ was used as an extractant. The extractant with soil at a ratio of 1:10 (soil/extractant) was added to 1 L water and was shaken for 15 minutes. The filtrate was collected, and the nitrate present was quantified by using IC.[39] The measured characteristics of the soil are given in Table 2.

Table 2. Characteristics of the Soil Used for Pot Trials

soil property	value
sand (%)	56.00 ± 0.89
silt (%)	33.00 ± 0.77
clay (%)	11.00 ± 0.85
organic matter (%)	2.05 ± 0.32
moisture (%)	30.00 ± 0.09
pH	6.56 ± 0.07
CEC ($cmol_c/kg$)	10.80 ± 0.53
available nitrate (mg/kg)	32.26 ± 0.88

2.5. Water-Holding Capacity of Soil in the Presence of LB. Two grams of LB was mixed with 200 g of the soil filled in a 250 mL polystyrene cup, installed with a filter paper (70 mm) at the bottom of the cup and some small holes to drain the excess water gravimetrically. Subsequently, the soil mixture was saturated with tap water and allowed to absorb the water for 24 h at 25 °C. A control experiment (in the absence of LB) was carried out. The water-holding capacity was measured as the percentage moisture present in the soil by using a moisture analyzer (MAX 5000XL, Arizona Instrument LLC, USA). The experiments were conducted in triplicate, and the average values were reported.

https://doi.org/10.1021/acsomega.2c07395
ACS Omega 2023, 8, 8427−8440

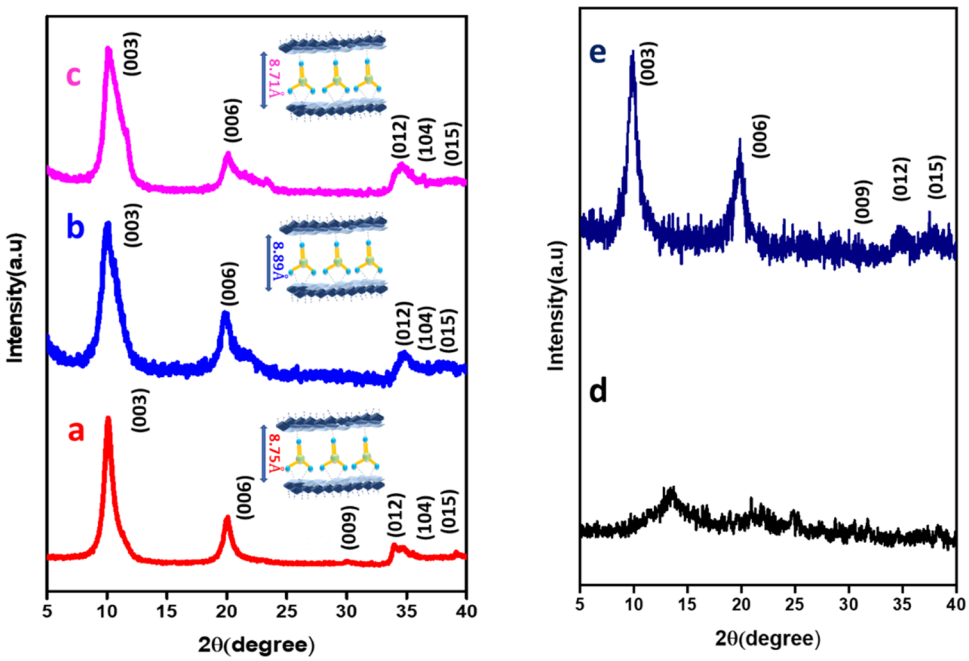

Figure 1. X-ray diffraction patterns of the synthesized nitrate forms of (a) Zn/Al LDH, (b) Mg/Al LDH, (c) Mg−Zn/Al LDH, (d) SA, and (e) LB.

2.6. Water Retention of Soil Using LB. Two grams of LB was mixed with 200 g of the soil filled in a 250 mL polystyrene cup with holes at the bottom and made 80% saturated by adding tap water and then weighed (C_1). The cup was stored at 25 °C. The weight of the cup was measured (C_2) every 2 days for a period of 12 days. A control experiment was carried out in the absence of LB. The water retention (WR%) was determined by using the following equation[40]

$$\mathrm{WR\%} = (C_2/C_1) \times 100 \quad (1)$$

The experiments were conducted in triplicate, and the average values were reported.

2.7. Nitrate Release from LDH and LB. The release studies of nitrate from the prepared materials were performed under different pH conditions (5.5 and 6.5) using tap water. The pH of tap water was adjusted using acetic acid (0.1 mol/L). The release studies were also conducted in a soil solution. To prepare the soil solution, 20 g of soil was mixed with 400 mL of deionized water with constant stirring at 300 rpm using a mechanical stirrer for 72 h followed by centrifugation at 6000 rpm for 30 min using a centrifuge (Nuve NF 800R, Ankara, Turkey). The supernatant solution was collected and used as a soil solution. The pH of the soil solution was measured as 6.5. All of the release studies were conducted at 25 °C.

In a typical release experiment, an LDH or LB of weight equivalent to 5 mg of nitrate was placed in tap water (or soil solution) in a reagent bottle (100 mL). The bottle was placed in a constant temperature water bath at 25 ± 1 °C and was shaken at 100 rpm. Aliquots of water samples (5 mL) were collected after 5, 10, 15, 30, 60, 120, 240, 480,1440, 2880, 4320, and 10080 min. The removed sample was replaced with 5 mL of fresh tap water or soil solution at the same pH to maintain a constant volume. The samples were filtered through a 45 μm (PVDF) syringe filter, and the filtrate was used to analyze the amount of released nitrate from Mg/Al, Zn/Al, Mg−Zn/Al LDH, and LB by using IC (Dionex ICS-5000$^+$ SP, Thermos Scientific, USA). The kinetics of nitrate release from Mg/Al, Zn/Al, Mg−Zn/Al LDH, and LB were compared to that of a soluble nitrate salt (KNO_3). To determine the buffering capacity of various LDH samples, the pH of the filtrate was measured at regular intervals. All release experiments were executed in triplicate, and average values were presented.

2.8. Pot Trials Using LDH and LB. The nitrate fertilizer efficiency of Mg/Al, Zn/Al, Mg−Zn/Al LDH, and LB was determined and compared to that of KNO_3 by growing coriander (*C. sativum*) in the soil collected and characterized (Table 2). The plant growth experiment was conducted in triplicate in a chamber under a controlled environment of temperature and light (25 °C and 2000 lumens). Coriander seeds were placed on paper towels, moistened with deionized water, and aged for 3 days at 25 °C to germinate the seeds. The soil (250 g) was filled in a 250 mL polystyrene cup with some small holes on the bottom. An amount of LDH with nitrate equivalent to 120 mg/kg was mixed with the soil uniformly. A control experiment was performed without adding any nitrate fertilizer. Coriander seeds were planted in each cup. To keep the K content equal in all of the pots in comparison to the pot with soluble KNO_3, a solution of KCl (4.89 mmol/L) was added to pots containing LDHs and LB. After germination, each pot was allowed to have 12 plants. The moisture level of the soil was kept at 70% by applying diionizedwater on a regular basis. Plants were harvested after 21 days and dried under an air oven at 65 °C, ground to powder using a ball mill, sieved through a 1 mm sieve, and stored in zip lock bags. Subsequently, nitrate assimilated by the plant was determined by the hot water method reported previously[41,42] using IC. The soil pH and the nitrate in the soil were also examined after 21 days.

3. RESULTS AND DISCUSSION

3.1. Characterization. Figure 1a−c shows X-ray diffractograms for nitrate forms of Zn/Al, Mg/Al, and Mg−Zn/Al LDHs. The XRD patterns exhibit well-defined peaks with high crystallinity for all of the LDHs. The basal spacing (d) calculated by utilizing Bragg's law ($n\lambda = 2d \sin\theta$) and using

https://doi.org/10.1021/acsomega.2c07395
ACS Omega 2023, 8, 8427−8440

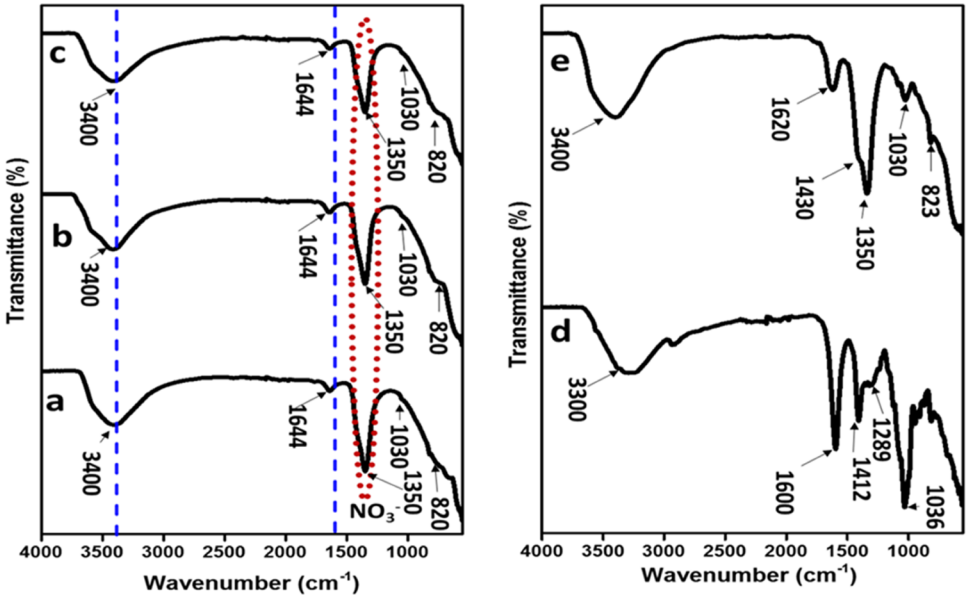

Figure 2. FTIR spectra of the synthesized nitrate-loaded (a) Zn/Al LDH, (b) Mg/Al LDH, (c) Mg−Zn/Al LDH, (d) SA, and (e) LB.

(003) reflection was 8.90, 8.89, and 8.89 Å, respectively, for Zn/Al, Mg/Al, and Mg−Zn/Al LDHs. It is widely known that the basal *d*-spacing obtained for various LDHs depends on the type of charge-balancing interlayer guest anion. The *d*-spacing of a nitrate LDH is expected to be higher than that of a carbonate LDH, which may be associated with stronger electrostatic interactions existing between the divalent carbonate interlayer anion and the host layer when compared to that of a monovalent nitrate anion and host layer.[43] As seen in Figure 1, the 003 basal reflection occurred at approximately 2θ = 10.02° corresponding to a *d*-spacing of 8.9 Å and an interlayer distance of 4.1 Å for synthetic LDHs with nitrate anion in the interlayer space, and this was consistent with findings for Zn/Al, Mg/Al, and Zn−Mg/Al LDHs. Olanrewaju et al.[43] reported a basal spacing of 8.8 Å for nitrate Mg−Al LDH prepared using ammonium nitrate in the absence of inert gases. According to the authors, the ammonium ions complex with carbonate ion in solution and prevents the formation of the carbonate form of LDH. They observed the formation of carbonate LDH when NaOH was used as a base for the synthesis. In our case, the synthesis under a nitrogen atmosphere and the presence of excess nitrate in the synthesis medium assisted the formation of the nitrate form of LDH, which is carbonate-free. A similar *d*-spacing of 8.84 Å was reported for nitrate Zn−Al LDH by Mahjoubi et al.,[44] where the synthesis was done by coprecipitation method using NaOH in the presence of excess nitrate anions. Shafigh et al.[45] prepared Zn−Mg/Fe LDH with nitrate in the interlayer and observed a basal *d*-spacing of 8.7 Å. A peak broadening was observed for the 003 basal peak for Mg/Al LDH and Mg−Zn/Al LDHs. Xiao et al.[46] prepared nitrate Mg−Zn/Al LDH by coprecipitation method for folic acid intercalation, and the pristine LDH exhibited the typical diffraction peaks with a basal spacing d_{003} of 8.8 Å and d_{006} of 4.5 Å. The observations were similar to the values obtained in this study. Although all of the prepared LDH materials showed a crystalline nature, Mg/Al LDH and Mg−Zn/Al LDH presented peak broadening for reflections. According to Ellis et al.,[47] disordered anions in the interlayer region that exist at various angles relative to the hydroxide sheets will result in the broadening of XRD peaks while well-ordered anions perpendicular to the hydroxide sheets will make sharp, intense peaks. The peak broadening could also be attributed to a structural disorder like stacking faults or Scherrer's broadening due to smaller crystallites leading to a decrease in crystallinity.[48] Since the basal distances observed in all three LDHs were similar, it might be fair to assume that the presence of Mg^{2+} ions in the brucite-like layer resulted in smaller LDH crystallites causing the broadening of XRD peaks in general.[48] Figure 1d displays the XRD pattern of sodium alginate with a characteristic peak at 14.28°, which indicated its amorphous nature, and the observation is in line with other reported studies.[49,50] The XRD pattern of LB (Figure 1) shows the characteristic peaks corresponding to 003, 006, and 012 reflections, and the d_{003} value was 8.9 Å, suggesting that the nitrate-loaded Mg/Al LDH was successfully encapsulated in alginate and the structure of LDH was not affected by the biopolymer matrix.[51]

To better understand the functional group compositions and confirm the existence of nitrate anions in the interlayer, the prepared materials were characterized by ATR-FTIR spectroscopy, and the spectra obtained are shown in Figure 2a−c. The spectra of Zn/Al, Mg/Al, and Mg−Zn/Al LDHs were similar. The broad band at 3400 cm^{-1} was attributed to the stretching vibration of the hydroxyl groups of the brucite-like layer and interlayer water. The corresponding bending mode of the hydroxyl groups of interlayer water molecules was observed at 1644 cm^{-1}. The band at 1350 cm^{-1} was assigned to the vibration modes (asymmetric stretch ν_3) of nitrate, which clearly indicated the effective intercalation of nitrate in the interlayer space. Free nitrate anion has a D_{3h} symmetry, which lowers for a nitrate anion confined in the LDH interlayer space due to interactions with water molecules and hydroxyl groups.[52] The distortion of the symmetry of nitrate ions in all of the LDH materials can be confirmed by the presence of a weak band around 1030 cm^{-1} (N−O symmetric stretching mode ν_1), which is not normally active in a free nitrate anion with a D_{3h} symmetry. The bands observed at 820 and 667 cm^{-1} were attributed to ν_2 (out-of-plane bending mode) and ν_4 (in-plane bending mode) of nitrate anion. Similar results were obtained by Benício et al.[53] and Cao et al.[54] for nitrate

https://doi.org/10.1021/acsomega.2c07395
ACS Omega 2023, 8, 8427−8440

Table 3. Elemental Composition Analysis Data

sample	Zn (wt %)	Mg (wt %)	Al (wt %)	x value calculated $(M^{3+}/(M^{2+} + M^{3+})$	stoichiometric ratio (M^{2+}/M^{3+})	AEC (mequiv/100 g)
Zn/Al LDH	32.17		9.57	0.23	3.36	337.3
Mg/Al LDH		19.78	9.73	0.33	2.03	339.6
Mg−Zn/Al LDH	22.1	10.13	10.1	0.23	3.19	336.8

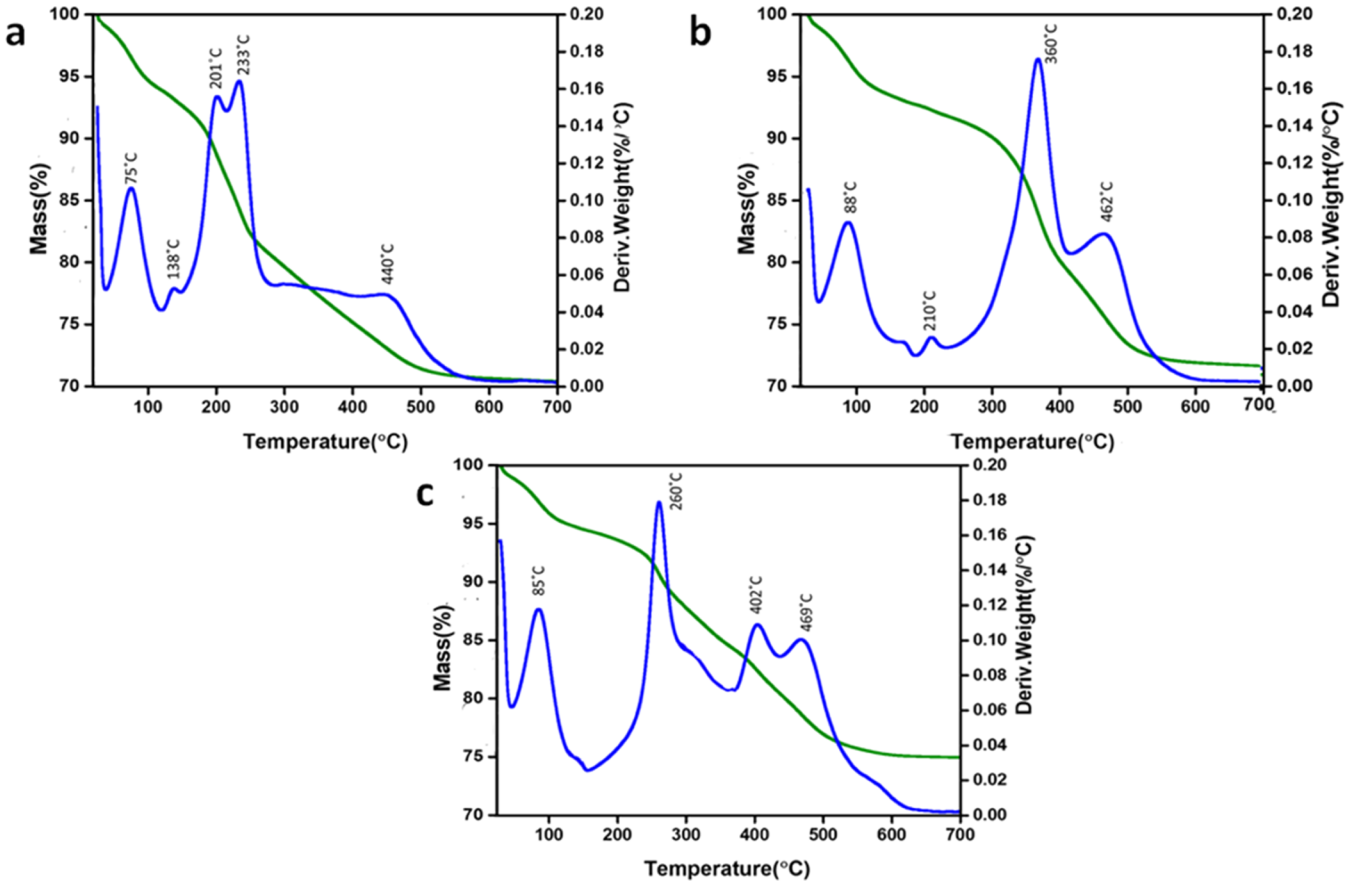

Figure 3. TGA curves of (a) Zn/Al LDH, (b) Mg/Al LDH, and (c) Mg−Zn/Al LDH.

Mg/Al LDH. However, the findings of Mahjoubi et al.[44] and Ravuru et al.[55] showed bands at 1380 cm^{-1} of nitrate anion in the interlayer using Zn/Al and Ni/Al LDH.

FTIR spectra of SA (Figure 2d) showed a broad band at 3300 cm^{-1} due to the stretching vibration of hydroxyl groups, whereas the bands at 1600 and 1412 cm^{-1} were ascribed to a stretching vibration (symmetric and asymmetric) of carboxylate groups; the stretching vibration of the C−O−C groups was observed at 1036 cm^{-1}.[56] FTIR spectra of LB (Figure 2e) demonstrated characteristic peaks of both Mg/Al LDH and SA; the bands at 1600 and 1420 cm^{-1} were attributed to the stretching SA functional groups, while the bands at 1350 and 823 cm^{-1} were associated with the vibration modes of Mg/Al LDH.

The results of the ICP-OES analysis for the metal element composition of various nitrate-intercalated LDHs are presented in Table 3.

The x values determined by ICP-OES were very close to the ideal range of proper LDH formation, i.e., $0.2 \leq x \leq 0.33$. However, it is to be noted that although the intended compositional ratio 2:1 for M^{2+}/M^{3+} was obtained only for Mg/Al LDH, Zn/Al LDH and Mg−Zn/Al LDH showed a cationic molar ratio of 3.36 and 3.19, respectively, within the ideal range of 2−4, indicating the formation of thermodynamically stable LDHs.[57] The chemical formula of various LDHs could be written as Zn/Al LDH-$[Zn_{0.77}^{2+}\ Al_{0.23}^{3+}\ (OH)_2]^{0.23+}\ (NO_3^-)_{0.23}{\cdot}0.5(H_2O)$, Mg/Al LDH-$[Mg_{0.67}^{2+}\ Al_{0.33}^{3+}\ (OH)_2]^{0.33+}(NO_3^-)_{0.33}{\cdot}0.5(H_2O)$, and Mg−Zn/Al LDH-$[Mg_{0.53}^{2+}\text{-}Zn_{0.24}^{2+}\ Al_{0.23}^{3+}\ (OH)_2]^{0.23+}\ (NO_3^-)_{0.23}{\cdot}0.5(H_2O)$ correspondingly. Based on the stoichiometric ratios, the short representation of the LDH formulations may be considered as Zn_3Al LDH, Mg_2Al LDH, and Zn_2MgAl LDH.

The AEC values determined for various LDHs (Table 3) showed similar values and were close to the theoretical AEC value of 326 $cmol_c/kg$ obtained for LDH with molecular formula $Mg_{0.67}Al_{0.33}(OH)_2(C_{10}H_{19}O_2)_{0.17}(C_{10}H_{19}O_2Na)_{0.01}(NO_3)_{0.01}(CO_3)_{0.05}{\cdot}0.42\ H_2O$.[58] The AEC of LDH is determined by the metal cation ratio, the ability of the interlayer anion in stabilizing the lamellar structure, and the molecular mass of the cations and anions involved. According to Leroux and Besse,[9] the AEC values of LDH might range between 200 and 450 $cmol_c/kg$ and are generally higher than the cation-exchange capacities, CECs, of typical montmorillonites. Values below 200 $cmol_c/kg$ are not feasible when the M^{2+} and M^{3+} ratios are very small to support the LDH structure. The presence of

https://doi.org/10.1021/acsomega.2c07395
ACS Omega 2023, 8, 8427−8440

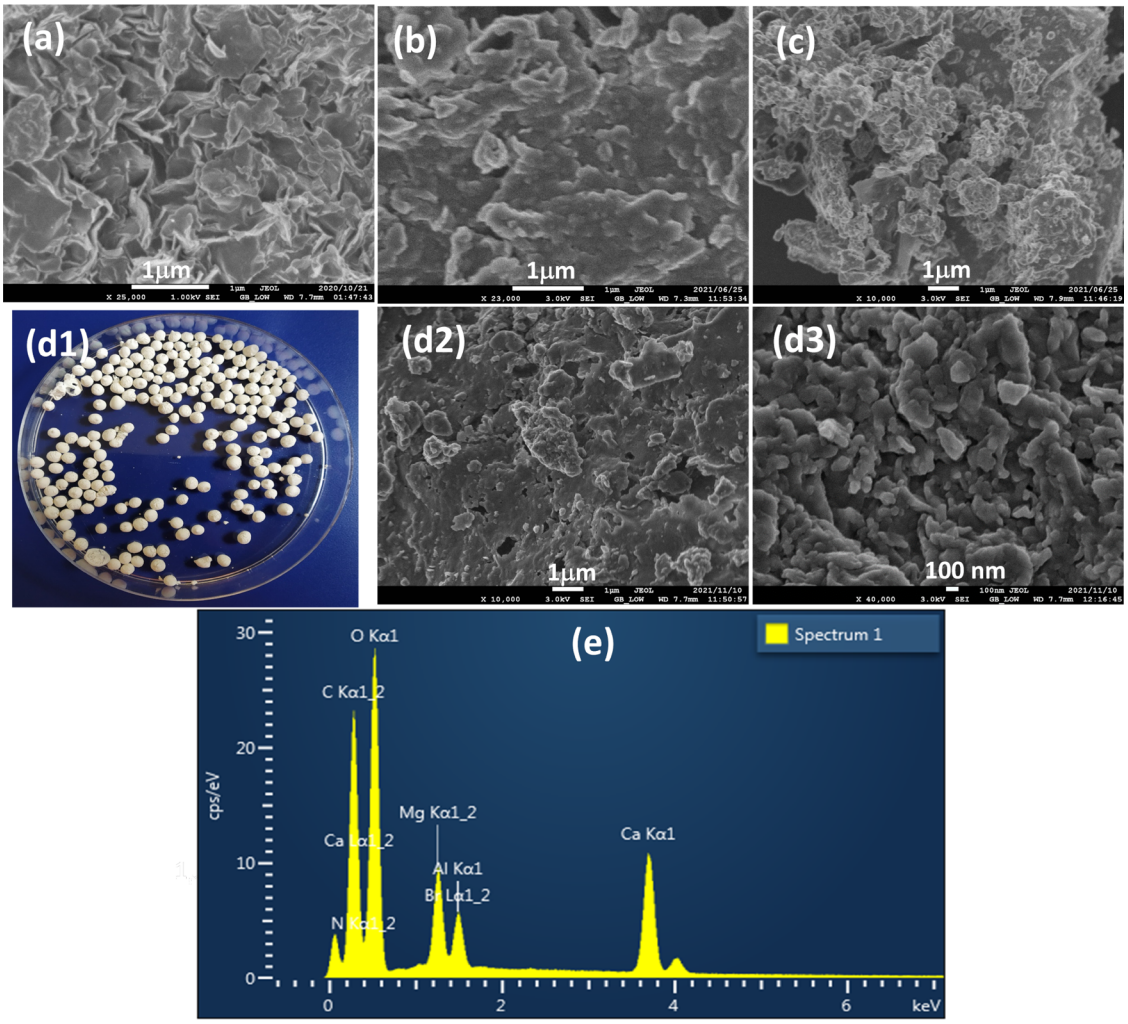

Figure 4. (a) SEM image of Zn/Al LDH, (b) SEM image of Mg/Al LDH, (c) SEM image of Mg−Zn/Al LDH, (d1) digital image of LB, (d2, d3) SEM image of LB at different magnifications (10× and 40×), and (e) EDS spectra of LB.

more readily exchangeable nitrate anion could also contribute to the reasonably high values of AEC observed in the prepared LDH materials.[59]

TGA analyses were utilized to examine the thermal decomposition profiles of nitrate-intercalated Zn/Al, Mg/Al, and Mg−Zn/Al LDH, and the thermograms are shown in Figure 3a−c. The TGA/DTG curves for Zn/Al LDH showed the first mass loss at 75 °C, which was attributed to the loss of the weakly adsorbed surface water.[60−62] The second mass loss was observed at 138 °C due to the removal of interlayer water. This was followed by the largest mass loss peak at 233 °C with a shoulder peak on the left accounting for about 20% mass loss. These peaks corresponded to the dehydroxylation of brucite-like layers where the shoulder peak at 201 °C represented Al−OH dehydroxylation, while the Zn−OH dehydroxylation occurred at 233 °C.[60] According to Yao et al.,[63] the dehydroxylation temperature of Al−OH is lower than that of Mg−OH. Additional mass loss registered around 440 °C could be attributed to the decomposition of nitrate to NO_2.[44,64] In the case of Mg/Al LDH, the DTG peak positions were at 88, 210, 360, and 462 °C, respectively, for surface water, interlayer water, hydroxyl groups, and nitrate removal. All of the peak positions were shifted to higher temperatures indicating higher thermal stability of Mg/Al LDH in comparison to that of Zn/Al LDH. Moreover, a single mass loss peak was observed for the dehydroxylation in this case, indicating an overlap of Al−OH and Mg−OH decompositions. The peak positions obtained for the respective decomposition steps for Mg−Zn/Al LDH were 85, 147, 260, 335, 402, and 469 °C, demonstrating similarities in thermal decomposition features of Zn/Al LDH and Mg/Al LDH. The peak positions suggested thermal stability closer to that of Mg/Al LDH. Considering the denitration occurring at a relatively higher temperature, the mass losses registered were 11, 17, and 16% for Zn/Al LDH, Mg/Al LDH, and Mg−Zn/Al LDH, respectively, which could be an indication of a lower concentration of nitrate anions in the interlayer of Zn/Al LDH when compared to the counterparts.

Magri et al.[65] observed that for Zn_2Al-CO_3, the onset temperature for dehydroxylation was observed at a lower temperature (215 °C) in comparison to Mg_2Al−CO_3 (282 °C) and thus inferred that the Mg_2Al−CO_3 structure is thermally more stable than the analogous phase of zinc and our observations are similar to these findings but on the nitrate-intercalated LDH. Monteiro et al.[66] prepared Mg/Al LDH nitrate as a precursor to prepare oxo molybdenum catecholate complexes and observed a similar thermal decomposition pattern for the pristine nitrate LDH. Wang et al.[67] closely

https://doi.org/10.1021/acsomega.2c07395
ACS Omega 2023, 8, 8427−8440

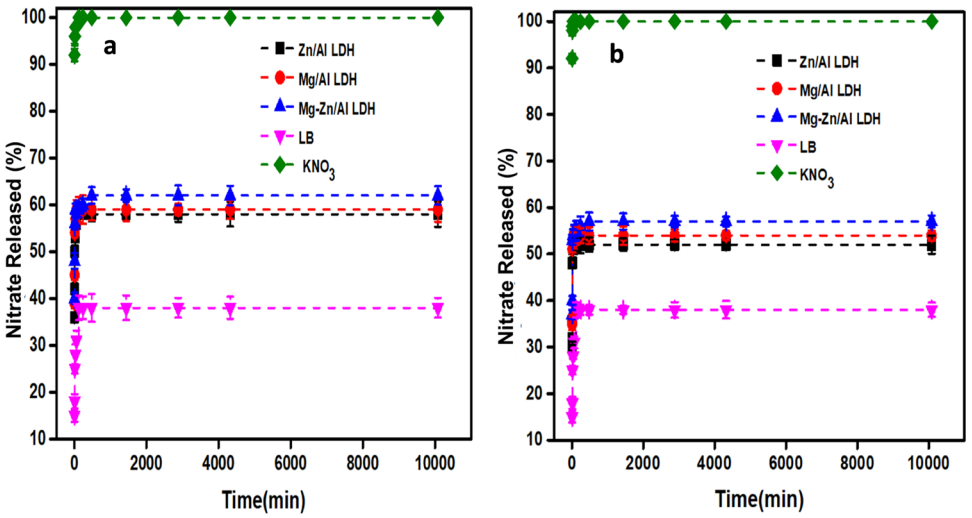

Figure 5. Nitrate release from various LDHs and LB in tap water at pH (a) 5.5 and (b) 6.5.

monitored the decomposition mechanism in nitrate-loaded Ni/Al LDH by the TG-DTG-MS study and concluded that the thermal decomposition of LDH proceeds in individual processes, i.e., removal of the physisorbed and interlayer waters, dehydroxylation of the layers, and decomposition of the interlayer nitrate ions (denitration) and the interlayer nitrate ions decompose only after the destruction of the lamellar LDH structure.

SEM images of Zn/Al, Mg/Al, and Mg−Zn/Al LDHs are shown in Figure 4a−c. LDHs exhibited a plate-like morphology[61,68] as expected. Zn/Al LDH displayed irregular lamellar structures composed of clearly distinguishable flake-like platelets. This sample showed the highest prevalence of flake-like structures among all three LDH samples, and the structure of these flakes was more defined in comparison to the other LDHs. These flakes were stacked in an orderly manner, and this observation was in agreement with the XRD results, which showed crystalline sharp peaks for Zn/AL LDH. On the other hand, Mg/Al LDH and Mg−Zn/Al LDH exhibited relatively smaller and more aggregated platelets, which were apparent from the XRD peak broadening observed. Considering the fact that various LDHs have similar Al^{3+} contents, it may be concluded that the incorporation of Mg^{2+} within the brucite-like layer causes more agglomeration of particles, which could be associated with the nucleation and growth mechanism of LDH in different reaction environments (metal salts).[69] The SEM observations agree with the previous reports[70,71] confirming that the substitution by transition metal varied the morphology of different LDHs and the platelet size increased upon Cu-, Co- and Zn-substitution.

Figure 4d shows the digital image of LB (Figure 4d1) and the SEM surface image of the alginate beads at two different magnifications (Figure 4d2,d3). The SEM micrograph of LB exhibits a porous nature. At higher magnifications, the LDH particles appeared to be covered by a polymer coating, which was characteristic of the biopolymer matrix, and this observation was similar to that reported by Prevot et al.[72] for Ni/Al LDH-alginate bionanocomposites synthesized by confined coprecipitation. EDS spectrum of LB indicated the existence of Mg and Al at 1.25 and 1.48 keV as Kα X-ray signals together with carbon, nitrogen, oxygen, and calcium (used for cross-linking) (Figure 4e).[32,73] These results indicated a close interaction of the Mg/Al LDH with the biopolymers, facilitating the homogeneous integration within the polymer matrix.

3.2. Nitrate Release Profiles of LDH and LB. The nitrate release from various LDHs and LB was studied to get an understanding of the slow-release properties. The release profiles obtained for the prepared materials in tap water at 25 °C under different pH conditions (pH 5.5 and 6.5) are shown in Figure 5a,b.

A 100% nitrate release was obtained for KNO_3 within 5 min, predictably as a soluble nitrate source. In the case of powder LDH samples, a bimodal release pattern was observed meaning a comparatively fast release until 60 min followed by a steady and slow release of nitrate anion thereafter. At pH 5.5, which simulates an acidic environment, about 55% of nitrate intercalated was released for Zn/Al LDH, whereas it was 61% for Mg/Al LDH and Mg−Zn Al LDH after 7 days leaving around 45 and 39% nitrates in the interlayer of the LDHs. The initial fast release observed can be attributed to the nitrate ions on the surface of LDH, which usually easily ion-exchange with hydroxyl or carbonate ions in the water.[74,75] LDH materials have an inherently high affinity for carbonate anions (as dissolved CO_2 in water or atmospheric CO_2), which can displace the intercalated nitrate very fast.[29] However, all three LDHs after the initial fast-release stage showed slower exchange leading to slow-release properties. Silva et al.[75] proposed that the interlayer ionic barrier played a vital role in the slow release of intercalated anions. The result of the initial exchange of nitrate with carbonate in solution resulted in the surface-adsorbed carbonate anion that could obstruct the release of intercalated nitrate, thus interrupting the quick release of nitrate ions. In a water medium at pH 6.5, the LDH materials released relatively less amount of nitrate after 7 days, which were 51, 53, and 57%, respectively, for Zn/Al LDH, Mg/Al LDH, and Mg−Zn/Al LDH. LDH structures are sensitive to the pH of the release environment, and a higher amount of nitrate release was expected at lower pH due to the partial dissolution of LDH layers.[76] The results demonstrated a pH-dependent release pattern for nitrate ions from LDH in an aqueous medium for a longer time period.

Among different LDHs, Mg−Zn/Al LDH showed a slightly higher amount of nitrate release after 7 days than the others, whereas Zn/Al LDH showed the lowest amount of release. As per the XRD results (Figure 1), Zn/Al LDH showed the

https://doi.org/10.1021/acsomega.2c07395
ACS Omega 2023, 8, 8427−8440

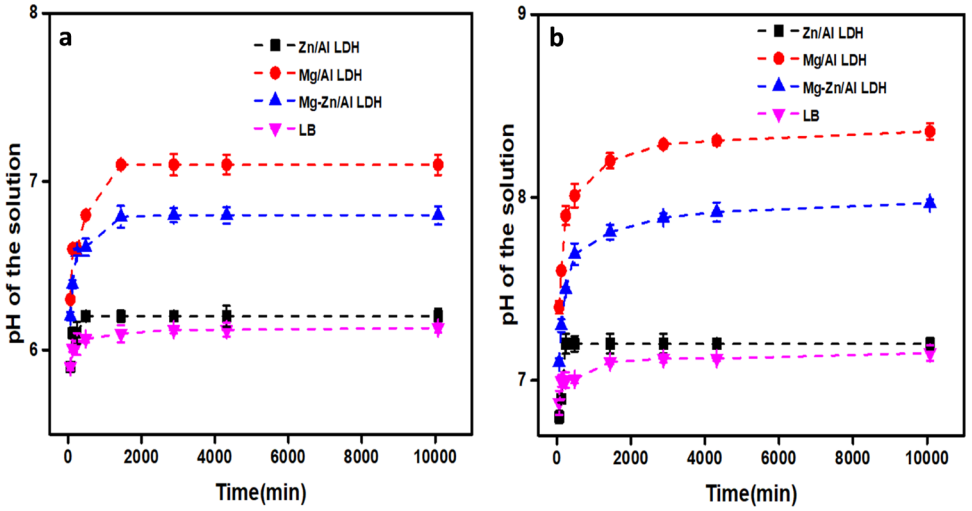

Figure 6. Buffering capacity of Zn/Al, Mg/Al, Mg−Zn/Al LDH, and LB with a starting pH of (a) 5.5 and (b) 6.5.

highest crystallinity, whereas the Mg-containing LDHs were less crystalline. The LDH with higher crystallinity is structurally more intact, which could result in the release of nitrate anions at a slower pace. According to Silva et al.,[75] the release rate depends on a few factors such as the material's crystallinity, the charge density of the layer, and the component used in the layer. The use of various M^{2+}/M^{3+} in this work verifies these factors, which demonstrated that Zn/Al LDH with higher crystallinity released nitrate anions slowly in comparison to the LDHs with lower crystallinity. The observations on nitrate release from Zn/Al LDH were similar to that reported by Nunes et al.,[29] where 50% release of nitrate was obtained 80 min in a water medium.

The nitrate release profiles of LB at pH 5.5 and 6.5 in an aqueous medium were similar and exhibited greater retaining (68%) and a much slower release of nitrate ions. This demonstrated the effective encapsulation offered by the biopolymer matrix to LDH in the composite bead sample. The biopolymer matrix provided a structural barrier for the nitrate anion diffusion as well as protected the LDH structure from exposure to different pH environments, further slowing down the release of nitrate. The observations are similar to that of Han et al.,[73] where Mg/Al LDH-alginate beads showed similar release patterns in phosphate medium at solution pH between 5.0 and 9.0.

The buffering capacities of various LDHs were also studied, and the results are presented in Figure 6. The pH increases observed for Zn/Al, Mg/Al, Mg−Zn/Al LDH, and LB at the end of the experiments were 6.15, 7.19, 6.88, and 6.08, respectively, when the starting pH was 5.5 and the values were 7.11, 8.26, 7.9, and 7.03 when the starting pH was 6.5. From the results, it was apparent that Zn/Al LDH had a lower buffering capacity, whereas Mg/Al LDH offered the highest buffering capacity among various LDHs. LB showed the lowest buffering capacity of all of the tested materials.

Borgiallo and Rojas[77] reported high pH buffering capacity for Ca−Al LDH with Friedel's salt structure and their utility as heavy metal scavengers. The high buffering capacity of Fe−Mg/Mn-LDH and maintenance of pH between 9 and 10 during nitrate adsorption and removal in aqueous solutions were reported by Zhou et al.,[78] as well. Sieda et al.[79] employed carbonate forms of Ca/Fe LDH and Mg/Fe LDH for phosphate removal from aqueous solutions and suggested that buffering the pH effect off LDH due to the release of metal cations (Mg^{2+}, Ca^{2+}, Fe^{3+}) and/or their hydroxides effectively assisted in phosphate removal. Since Mg^{2+} forms stronger ionic bonds with hydroxyl groups,[80] it was fair to expect a higher buffering capacity for Mg/Al LDH than for Zn/Al LDH, which was also confirmed by the buffering capacity order Mg/Al LDH > Mg−Zn/Al LDH > Zn/Al LDH observed in this study.

The biphasic release of nitrate from Zn/Al, Mg/Al, Mg−Zn/Al LDHs, and LB was also observed in soil solution, which progressed slowly over 7 days and reached 61.25, 64, 69, and 40.51%, respectively, while KNO_3 showed a constant release as expected (Figure 7). As reported in the literature, the anion-

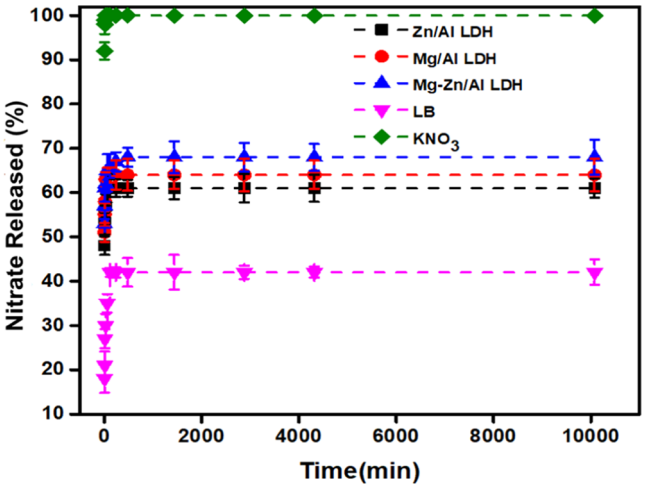

Figure 7. Nitrate release profiles of various LDHs in soil solution.

exchange selectivity order for LDH is CO_3^{2-} > HPO_4^{2-} > SO_4^{2-} > Cl^- > NO_3^-.[81,82] Higher exchangeability of carbonate with nitrate in a simulated soil medium was reported by Dorante et al.[79] However, in agricultural soil, bicarbonate ion is the predominant anion, whereas the concentration of carbonate ion is significantly low.[83] Ureña-Amate and co-workers[84] reported similar observations on soil solution where the 50% nitrate released was higher for the simulated soil solution medium than for the decarbonated water medium. Berber et al.[85] demonstrated that in a neutral soil solution, 70%

https://doi.org/10.1021/acsomega.2c07395
ACS Omega 2023, 8, 8427−8440

of nitrate was released from Mg/Al LDH within 8 days, which was in agreement with the observations of the present study.

Nitrate release studies also indicated that the composite bead LB was capable of retaining a higher amount of nitrate at both pH conditions, demonstrating a significantly slower release rate when compared to LDH alone in powder form. Composite beads not only avoid difficulties in terms of the application of powder form of LDH in soil but also protect from the low pH environment if the soil is unfavorably acidic.

3.3. Water-Holding Capacity of Soil Using LB. The water-holding capacity of the soil was analyzed using a moisture analyzer after 24 h of water saturation, and the result demonstrated that the water-holding capacity of soil increased up to 1.5 times in the presence of LB than in the control experiment. The moisture content of the soil in the presence of LB was 46.2%, whereas that of the untreated soil was 30%. LB could increase the water-holding capacity of soil and establish a favorable condition for the plant to uptake the nutrients. Wang et al.[26] prepared calcium alginate beads impregnated with ball-milled biochar as a new type of water/nutrient retention agent. The cumulative swelling and release characteristics of water and nitrate indicated that the beads have great potential as a soil amendment to improve their nutrient retention and water-holding capacity. In a very recent study, van der Merwe et al.[86] used industrial kelp solid waste-extracted alginate slurries to prepare amendment beads to improve water retention slow-release properties. In addition to improving water-holding capacity, hydrogel beads are reported to enhance the other properties of soil such as increasing infiltration rates, reducing compaction tendency, increasing plant performance, and increasing soil aeration, which some or other ways are beneficial to plant growth.[87]

3.4. Water Retention of Soil Using LB. Water retention tests were conducted with LB over 12 days, and the results are presented in Figure 8. It can be seen from the figure that the water retention capacity of soil gradually decreased in the control experiment gradually over 12 days; only 6.2% of the water remained in the soil at the end of the experiment cycle. On the other hand, 26% of water remained in the soil with LB, indicating that LB can increase the water retention properties of soil and help maintain soil moisture levels over extended periods. Previous research into the water absorption and retention capacity of hydrogels in general and alginate-based hydrogels in particular show potential for using hydrogels in the field of soil amendments.[82] Taha et al.[88] employed alginate-immobilized ureolytic bacteria for maximizing water retention in soil. The water uptake measurements showed that alginate beads retain 55% more water in the soil. Liu et al.[89] reported that the water retention of the mixed soil (sandy soil: loam soil = 3:1; 25 mesh) improved in the presence of cellulose nanofiber-impregnated alginate-poly(vinyl alcohol) hydrogel beads. According to the authors, the closer three-dimensional network in the biopolymer matrix accommodated water molecules, which could be released later into the soil by the diffusion process.

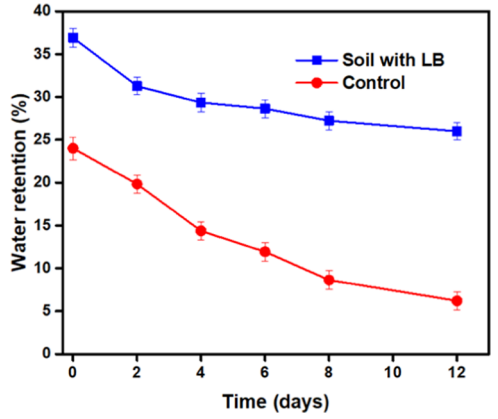

Figure 8. Water retention of soil with and without LB.

3.5. Nitrate Assimilation by Coriander. To evaluate the potential of various LDHs and LB slow-release fertilizers realistically, pot trials were conducted using coriander (*C. sativum*) seeds and the results were compared to the performance of soluble nitrate source KNO_3 and are reported in Figure 9. The data obtained on the effect of Zn/Al LDH, Mg/Al LDH, Mg−Zn/Al LDH, LB, and KNO_3 on soil and plant characteristics are presented in Table 4. The amount of dry matter produced after harvest is shown in Figure 10.

The nitrate in the soil was significantly lower for LB-containing pot, and the results demonstrated that the nitrate availability in the soil was significantly higher in pots containing LDHs. The lower concentration of nitrate in the pot containing LB is in agreement with the nitrate release study results where LB retained a substantial amount of nitrate in the biopolymer matrix resulting in a much slower release rate when compared to LDHs in powder form. The nitrate present was low in the soil where KNO_3 was added as a fertilizer, which indicated the quick release of nitrate from the soluble source and the mineralization and leaching occurring thereafter. The results indicated that LDHs could retain a higher amount of nitrate in the soil through slow release for 21 days, thereby preventing leaching. LDHs were able to retain nitrate for soil fertility, leaving it available for use in the future.

Figure 9 shows the coriander plant after 18 days of growth with different LDHs, LB treatments against the control. A comparison of the pictures clearly showed increased plant growth with LDH treatment when compared to the control although the pot with KNO_3 showed a slightly better growth of plants. Figure 10 compares dry matter production with and without the LDH and LB materials. Regardless of the nitrate present in the soil, the dry matter was significantly lower with LB than with any LDH or KNO_3. This is consistent with the release pattern documented in Figure 7. Although Mg−Zn/Al LDH showed the highest release rate in water and soil solutions, the nitrate release from LDHs was similar in the soil conditions. Considering the complexity and inhomogeneity of soil, such slight variations can be justified. The dry matter production was the lowest in the control, which was probably due to lower water-holding capacity and lower anion-exchange capacity.

The nitrate uptake by the plant was measured by the nitrate present in the dry matter. The values obtained were 4.78, 4.83, 4.80, 3.61, and 5.02 mg/pot, respectively, for Zn/Al LDH, Mg/Al LDH, Mg−Zn/Al LDH, LB, and KNO_3. The results clearly indicated that LDHs were capable of supplying nitrate effectively to the plant similar to KNO_3. Another significant advantage for LDHs was the ability to increase the soil pH. A higher pH value was acquired when LDHs were utilized as a fertilizer for coriander. Plants release a H^+ ion or excrete an OH^- ion when taking up a nitrate ion that can increase the pH at the root zone, which may be the reason for increasing the soil pH after using KNO_3. The increase in soil pH by the use of

https://doi.org/10.1021/acsomega.2c07395
ACS Omega 2023, 8, 8427−8440

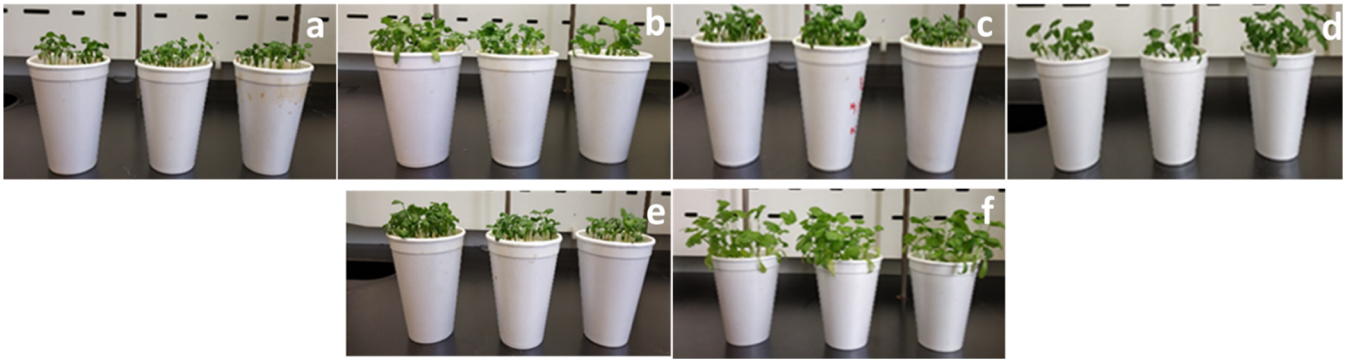

Figure 9. Growth of coriander 18 days after sowing: (a) control, (b) Zn/Al LDH, (c) Mg/Al LDH, (d) M−Zn/Al LDH, (e) LB, and (f) KNO_3. Digital images were taken by ASR, the first author of this article.

Table 4. Soil and Plant Characteristics after Harvest

sample	soil pH	available nitrate in soil (mg/pot)	nitrate content in dry matter (mg/pot)
Zn/Al LDH	7.25 ± 0.02	10.25 ± 0.68	4.782 ± 0.15
Mg/Al LDH	8.12 ± 0.03	9.82 ± 0.55	4.828 ± 0.16
Mg−Zn/Al LDH	7.89 ± 0.05	9.91 ± 0.72	4.802 ± 0.24
LB	6.92 ± 0.02	5.35 ± 0.51	3.610 ± 0.13
KNO_3	6.72 ± 0.04	6.70 ± 0.88	5.021 ± 0.44
control	6.51 ± 0.01	2.93 ± 0.02	3.121 ± 0.04

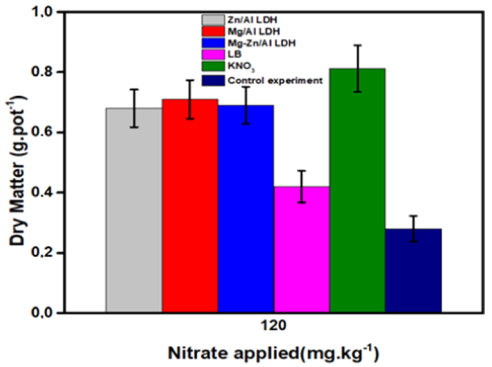

Figure 10. Dry matter production of coriander after 21 days.

LDHs could be due to the anion exchange between the anions present in the soil and nitrate. The increase in soil pH diminishes the uptake of nitrate by the mineral phase of the soil and enhances the accessibility of nitrate to the plants.[83] In the case of low soil pH, the positive charges on soil particle surfaces can tightly retain negatively charged nutrients such as nitrate, potentially reducing the uptake by the plant. An increased soil pH can change the soil particle surface properties and thus increase the bioavailability of nitrate to the plant.[90]

In the case of LB, the nitrate assimilation was lower in comparison to LDHs in powder form. The decreased surface area of LB is not the only reason behind these properties, as Everaert et al.[11] reported that there was no significant difference between the powdered or granulated form of LDH toward the phosphor ion uptake. The physical barrier offered by the alginate prevents the LDH from exposure to the soil. Moreover, the alginate also forms an electrostatic obstruction that decreases the exchange rate of nitrate with other anions. This experiment demonstrated that the coriander growth was almost equal in pots containing LDHs compared to the pot with the soluble nitrate fertilizer. Moreover, the nitrate availability in the soil and soil pH increased significantly with the application of LDHs, demonstrating their capacity for soil conditioning and preventing the leaching of nitrate through the soil.

4. CONCLUSIONS

Various LDHs (Zn/Al LDH, Mg/Al LDH, Mg−Zn/Al LDH) with nitrate interlayer anions were successfully synthesized, and the nitrate release properties under different conditions were compared to KNO_3. To study the effect of biopolymer encapsulation on the release properties of LDH, composite beads were prepared by impregnating Mg/Al LDH in an alginate matrix. Physicochemical characterization revealed the effective intercalation of nitrate anions and the increased thermal stability of the Mg-containing LDHs. The release rate of nitrate ions from LDHs and LB in tap water and soil solution showed slow-release nature, and Mg/Al LDH showed the highest pH buffering capacity. The materials were employed as slow-release fertilizers for coriander growth. LDHs showed similar effectiveness for plant growth and produced dry matter that contained nitrate similar to that of soluble fertilizer. LDHs also increased the soil pH value, which enhanced the accessibility of nitrate to the plant. Although LB was able to hold water and able to retain nitrate for more extended periods, it showed lower productivity than the powder form of LDHs and KNO_3 for coriander growth since the nitrate release rate was much slower. The findings demonstrated the potential of LDHs as slow-release fertilizers, as reliable matrices to retain nitrate levels and soil pH and to avoid nitrate leaching. Encapsulation of LDH showed further reduction in the release rate, which supports its usage as a long-term crop fertilizer. Though this study has shown that LDHs can undoubtedly be a slow-release fertilizer with minimal harm to the environment, more lab-scale, long-term field, and commercial trials are required to establish the full potential of these materials. The use of LDHs in the powder form could be challenging on a large scale in assuring uniform distribution in the soil under field conditions. There is also a need to assess the performance of these materials against slow-release products available in the market for a proper efficacy comparison. The study also illustrates the need for further research to apply LDHs for different crops and cropping conditions to realize the full potential and design limitations of these materials as new-generation fertilizer adjuvants. Future work will be focused on establishing the size uniformity of the

https://doi.org/10.1021/acsomega.2c07395
ACS Omega 2023, 8, 8427−8440

LDHs, optimizing application strategies of LDHs for different cropping requirements as well as understanding the chemical transformation of the materials under soil conditions.

AUTHOR INFORMATION

Corresponding Author

Suprakas Sinha Ray − *Department of Chemical Sciences, University of Johannesburg, Doornfontein 2028 Johannesburg, South Africa; Centre for Nanostructures and Advanced Materials, DSI-CSIR Nanotechnology Innovation Centre, Council for Scientific and Industrial Research, Pretoria 0001, South Africa;* orcid.org/0000-0002-0007-2595; Email: rsuprakas@csir.co.za, ssinharay@uj.ac.za

Authors

Abhinandan Singha Roy − *Department of Chemical Sciences, University of Johannesburg, Doornfontein 2028 Johannesburg, South Africa; Centre for Nanostructures and Advanced Materials, DSI-CSIR Nanotechnology Innovation Centre, Council for Scientific and Industrial Research, Pretoria 0001, South Africa;* orcid.org/0000-0002-6464-605X

Sreejarani Kesavan Pillai − *Centre for Nanostructures and Advanced Materials, DSI-CSIR Nanotechnology Innovation Centre, Council for Scientific and Industrial Research, Pretoria 0001, South Africa;* orcid.org/0000-0001-8015-2941

Complete contact information is available at: https://pubs.acs.org/10.1021/acsomega.2c07395

Notes

The authors declare no competing financial interest.

ACKNOWLEDGMENTS

The authors are grateful to the CSIR (C6A0058) and the Department of Science and Innovation (C6EEM29) South Africa. ASR is thankful to the University of Johannesburg for the financial support (Student No. 219053157).

REFERENCES

(1) Widowati, L. R.; De Neve, S.; Setyorini, D.; Kasno, A.; Sipahutar, I. A.; et al. Nitrogen balances and nitrogen use efficiency of intensive vegetable rotations in South East Asian tropical Andisols. *Nutr. Cycling Agroecosyst.* **2011**, *91*, 131−143.

(2) Torres-Dorante, L. O.; Lammel, J.; Kuhlmann, H. Use of a layered double hydroxide (LDH) to buffer nitrate in soil: Long-term nitrate exchange properties under cropping and fallow conditions. *Plant Soil.* **2009**, *315*, 257−272.

(3) Shareef, M.; Gui, D.; Zeng, F.; Waqas, M.; Ahmed, Z.; Zhang, B.; Iqbal, H.; Xue, J. Nitrogen leaching, recovery efficiency, and cotton productivity assessments on desert-sandy soil under various application methods. *Agric. Water Manag.* **2019**, *223*, No. 105716.

(4) Norton, J.; Ouyang, Y. Controls and adaptive management of nitrification in agricultural soils. *Front. Microbiol.* **2019**, *10*, No. 1931.

(5) Kühling, I.; Beiküfner, M.; Vergara, M.; Trautz, D. Effects of adapted N-fertilisation strategies on nitrate leaching and yield performance of arable crops in North-Western Germany. *Agronomy* **2021**, *11*, 64.

(6) Ransom, C. J.; Jolley, V. D.; Blair, T. A.; Sutton, L. E.; Hopkins, B. G. Nitrogen release rates from slow-and controlled-release fertilizers influenced by placement and temperature. *PLoS One* **2020**, *15*, No. e0234544.

(7) El-Hout, N. M.; Fountain, J. W. Nitrogen release from polymer-coated urea: Effect of seasons and growing degree-days. *Crops Soils* **2021**, *54*, 23−31.

(8) Singha Roy, A.; Pillai, S. K.; Ray, S. S. Layered double hydroxides for sustainable agriculture and environment: An overview. *ACS Omega* **2022**, *7*, 20428.

(9) Leroux, F.; Besse, J. P. Layered Double Hydroxide/Polymer Nanocomposites. In *Interface Science and Technology*; Elsevier, 2004; Vol. *1*, pp 459−495.

(10) Everaert, M.; Warrinnier, R.; Baken, S.; Gustafsson, J. P.; De Vos, D.; Smolders, E. Phosphate-exchanged Mg−Al layered double hydroxides: A new slow release phosphate fertilizer. *ACS Sustainable Chem. Eng.* **2016**, *4*, 4280−4287.

(11) Everaert, M.; Degryse, F.; McLaughlin, M.J.; De Vos, D.; Smolders, E. Agronomic effectiveness of granulated and powdered P-exchanged Mg−Al LDH relative to struvite and MAP. *J. Agric. Food Chem.* **2017**, *65*, 6736−6744.

(12) Bukhtiyarova, M. V. A review on effect of synthesis conditions on the formation of layered double hydroxides. *J. Solid State Chem.* **2019**, *269*, 494−506.

(13) Wijitwongwan, R. P.; Intasa-ard, S.; Ogawa, M. Preparation of layered double hydroxides toward precisely designed hierarchical organization. *ChemEngineering* **2019**, *3*, 68.

(14) Wei, C.; Yan, X.; Zhou, Y.; Xu, W.; Gan, Y.; Zhang, Y.; Zhang, N. Morphological control of layered double hydroxides prepared by co-precipitation method. *Crystals* **2022**, *12*, 1713.

(15) Yang, B.; Wang, M.; Hu, X.; Zhou, T.; Zang, Z. Highly efficient semitransparent CsPbIBr2 perovskite solar cells via low-temperature processed In2S3 as electron-transport-layer. *Nano Energy* **2019**, *57*, 718−727.

(16) Zhao, S.; Cai, W.; Wang, H.; Zang, Z.; Chen, J. All-inorganic lead-free perovskite (-like) single crystals: Synthesis, properties, and applications. *Small Methods* **2021**, *5*, No. 2001308.

(17) Zhao, S.; Mo, Q.; Cai, W.; Wang, H.; Zang, Z. Inorganic lead-free cesium copper chlorine nanocrystal for highly efficient and stable warm white light-emitting diodes. *Photonics Res.* **2021**, *9*, 187−192.

(18) Benício, L. P. F.; Constantino, V. R. L.; Pinto, F. G.; Vergütz, L.; Tronto, J.; da Costa, L. M. Layered double hydroxides: new technology in phosphate fertilizers based on nanostructured materials. *ACS Sustainable Chem. Eng.* **2017**, *5*, 399−409.

(19) Mitter, N.; Worrall, E. A.; Robinson, K. E.; Li, P.; Jain, R. G.; Taochy, C.; Fletcher, S. J.; Carroll, B. J.; Lu, G. Q.; Xu, Z. P. Clay nanosheets for topical delivery of RNAi for sustained protection against plant viruses. *Nat. Plants* **2017**, *3*, No. 16207.

(20) Hatami, H.; Fotovat, A.; Halajnia, A. Comparison of adsorption and desorption of phosphate on synthesized Zn-Al LDH by two methods in a simulated soil solution. *Appl. Clay Sci.* **2018**, *152*, 333−341.

(21) López-Rayo, S.; Imran, A.; Bruun Hansen, H. C.; Schjoerring, J. K.; Magid, J. Layered double hydroxides: potential release-on-demand fertilizers for plant zinc nutrition. *J. Agric. Food Chem.* **2017**, *65*, 8779−8789.

(22) Mohammadi, M.; Mohammadi Torkashvand, A.; Biparva, P.; Esfandiari, M. The ability of layered double hydroxides for nitrate absorption and desorption in crop and fallow rotation. *Global J. Environ. Sci.* **2021**, *7*, 59−78.

(23) Chu, L.; Zhang, C.; Yu, J.; Sun, X.; Zhou, X.; Zhang, Y. Adsorption of nitrate from interflow by the Mg/Fe calcined layered double hydroxides. *Water Sci. Technol.* **2022**, *86*, 511−529.

(24) Kamimoto, Y.; Okamoto, N.; Hagio, T.; Yong-Jun, J.; Deevanhxay, P.; Ichino, R. Development of magnesium−iron layered double hydroxide and application to nitrate removal. *SN Appl. Sci.* **2019**, *1*, No. 1399.

(25) Halajnia, A.; Oustan, S.; Najafi, N.; Khataee, A. R.; Lakzian, A. The adsorption characteristics of nitrate on Mg−Fe and Mg−Al layered double hydroxides in a simulated soil solution. *Appl. Clay Sci.* **2012**, *70*, 28−36.

(26) Berber, M. R.; Hafez, I. H.; Minagawa, K.; Mori, T. A sustained controlled release formulation of soil nitrogen based on nitrate-layered double hydroxide nanoparticle material. *J. Soils Sediments* **2014**, *14*, 60−66.

(27) Halajnia, A.; Oustan, S.; Najafi, N.; Khataee, A. R.; Lakzian, A. Effects of Mg-Al layered double hydroxide on nitrate leaching and nitrogen uptake by maize in a calcareous soil. *Commun. Soil Sci. Plant Anal.* **2016**, *47*, 1162−1175.
(28) de Castro, G. F.; Ferreira, J. A.; Eulálio, D.; de Souza, S. J.; Novais, S. V.; Novais, R. F.; Pinto, F. G.; Tronto, J. Layered double hydroxides: matrices for storage and source of boron for plant growth. *Clay Miner.* **2018**, *53*, 79−89.
(29) Nunes, V. L. N.; Mulvaney, R. L.; Cantarutti, R. B.; Pinto, F. G.; Tronto, J. Improving nitrate fertilization by encapsulating Zn-Al Layered Double Hydroxides in alginate beads. *Nitrogen* **2020**, *1*, No. 11.
(30) Bokkhim, H.; Bansal, N.; Grøndahl, L.; Bhandari, B. Characterization of alginate−lactoferrin beads prepared by extrusion gelation method. *Food Hydrocolloids* **2016**, *53*, 270−276.
(31) Wang, B.; Gao, B.; Zimmerman, A. R.; Zheng, Y.; Lyu, H. Novel biochar-impregnated calcium alginate beads with improved water holding and nutrient retention properties. *J. Environ. Manage.* **2018**, *209*, 105−111.
(32) Karthikeyan, P.; Meenakshi, S. Development of sodium alginate@ZnFe-LDHs functionalized beads: Adsorption properties and mechanistic behaviour of phosphate and nitrate ions from the aqueous environment. *Environ. Chem. Ecotoxicol.* **2021**, *3*, 42−50.
(33) Vu, C. T.; Wu, T. MgAl-layered double hydroxides/sodium alginate beads for nitrate adsorption from groundwater and potential use as a slow-release fertilizer. *J. Clean. Prod.* **2022**, *379*, No. 134508.
(34) Ito, M. Improvement of nitrate-leaching control technology using an anion exchange compound on agriculture 1: synthesis of a Mg-Fe system layered double hydroxide and its anion exchange characteristics. *Soil Sci. Plant Nutr.* **2018**, *64*, 123−129.
(35) Bouyoucos, G. J. Hydrometer method improved for making particle size analyses of soils 1. *Agron. J.* **1962**, *54*, 464−465.
(36) Okalebo, J. R.; Gathua, K. W.; Woomer, P. L. *Laboratory Methods of Soil and Plant Analysis: A Working*, 2nd ed.; Sacred Africa: Nairobi, 2002; Vol. *21*, pp 25−26.
(37) Pleysier, J. L.; Juo, A. S. R. A single-extraction method using silver-thiourea for measuring exchangeable cations and effective CEC in soils with variable charges. *Soil Sci.* **1980**, *129*, 205−211.
(38) Schulte, E. E.; Hoskins, B.Recommended Soil Organic Matter Tests. In *Recommended Soil Testing Procedures for the North Eastern USA*; Northeastern Regional Publication, 1995; Vol. *493*, pp 52−60.
(39) Griffin, G.; Jokela, W.; Ross, D.; Pettinelli, D.; Morris, T.; Wilf, A. Recommended Soil Nitrate-N Tests. In *Recommended Soil Testing Procedures for the Northeastern United States*; Northeastern Regional Publication, 1995; Vol. *493*.
(40) Wu, L.; Liu, M. Preparation and properties of chitosan-coated NPK compound fertilizer with controlled-release and water-retention. *Carbohydr. Polym.* **2008**, *72*, 240−247.
(41) Konieczyński, P.; Wesołowski, M. Analysis of nitrate nitrogen in leaves and roots with rhizomes of medicinal plants. *Ann. Univ. Mariae Curie-Sklodowska Sect. DDD Pharm.* **2011**, *24*, 105−111.
(42) Novaes, H. B.; Vaitsman, D. S.; Dutra, P. B.; Pérez, D. V. Determination of nitrate in lettuce by ion chromatography after microwave water extraction. *Quim. Nova.* **2009**, *32*, 1647−1650.
(43) Olanrewaju, J.; Newalkar, B. L.; Mancino, C.; Komarneni, S. Simplified synthesis of nitrate form of layered double hydroxide. *Mater. Lett.* **2000**, *45*, 307−310.
(44) Mahjoubi, F. Z.; Khalidi, A.; Abdennouri, M.; Barka, N. Zn−Al layered double hydroxides intercalated with carbonate, nitrate, chloride and sulphate ions: Synthesis, characterisation and dye removal properties. *J. Taibah Univ. Sci.* **2017**, *11*, 90−100.
(45) Shafigh, M.; Hamidpour, M.; Furrer, G. Zinc release from Zn-Mg-Fe (III)-LDH intercalated with nitrate, phosphate and carbonate: The effects of low molecular weight organic acids. *Appl. Clay Sci.* **2019**, *170*, 135−142.
(46) Xiao, R.; Wang, W.; Pan, L.; Zhu, R.; Yu, Y.; Li, H.; Liu, H.; Wang, S. L. A sustained folic acid release system based on ternary magnesium/zinc/aluminum layered double hydroxides. *J. Mater. Sci.* **2011**, *46*, 2635−2643.
(47) Ellis, J. E.; Kim, K. J.; Cvetic, P. C.; Ohodnicki, P. R. In situ growth and interlayer modulation of layered double hydroxide thin films from a transparent conducting oxide precursor. *Cryst. Growth Des.* **2021**, *21*, 1518−1526.
(48) Thomas, G. S.; Kamath, P. V. Line broadening in the PXRD patterns of layered hydroxides: The relative effects of crystallite size and structural disorder. *J. Chem. Sci.* **2006**, *118*, 127−133.
(49) Karthikeyan, P.; Banu, H. A. T.; Meenakshi, S. Synthesis and characterization of metal loaded chitosan-alginate biopolymeric hybrid beads for the efficient removal of phosphate and nitrate ions from aqueous solution. *Int. J. Biol. Macromol.* **2019**, *130*, 407−418.
(50) Ionita, M.; Pandele, M. A.; Iovu, H. Sodium alginate/graphene oxide composite films with enhanced thermal and mechanical properties. *Carbohydr. Polym.* **2013**, *94*, 339−344.
(51) Xu, J.; Song, Y.; Zhao, Y.; Jiang, L.; Mei, Y.; Chen, P. Chloride removal and corrosion inhibitions of nitrate, nitrite-intercalated MgAl layered double hydroxides on steel in saturated calcium hydroxide solution. *Appl. Clay Sci.* **2018**, *163*, 129−136.
(52) Lainé, M.; Liao, Y.; Varenne, F.; Picot, P.; Michot, L. J.; Barruet, E.; Geertsen, V.; Thill, A.; Pelletier, M.; Brubach, J. B.; Roy, P.; Le Caër, S. Tuning the nature of the anion in hydrated layered double hydroxides for H2 production under ionizing radiation. *ACS Appl. Nano Mater.* **2018**, *1*, 5246−5257.
(53) Benício, L. P. F.; Eulálio, D.; Guimarães, L. D. M.; Pinto, F. G.; Costa, L. M. D.; Tronto, J. Layered double hydroxides as hosting matrices for storage and slow release of phosphate analyzed by stirred-flow method. *Mater. Res.* **2018**, *21*, No. e20171004.
(54) Cao, Y.; Fang, S.; Chen, K.; Qi, H.; Zhang, X.; Huang, C.; Wang, J.; Liu, J. Insight into the preparation of MgAl-Layered Double Hydroxide (LDH) intercalated with nitrates and chloride adsorption ability study. *Appl. Sci.* **2022**, *12*, 4492.
(55) Ravuru, S. S.; Jana, A.; De, S. Synthesis of NiAl-layered double hydroxide with nitrate intercalation: Application in cyanide removal from steel industry effluent. *J. Hazard. Mater.* **2019**, *373*, 791−800.
(56) Larosa, C.; Salerno, M.; de Lima, J. S.; Meri, R. M.; da Silva, M. F.; de Carvalho, L. B.; Converti, A. Characterisation of bare and tannase-loaded calcium alginate beads by microscopic, thermogravimetric, FTIR and XRD analyses. *Int. J. Biol. Macromol.* **2018**, *115*, 900−906.
(57) Cavani, F.; Trifiro, F.; Vaccari, A. Hydrotalcite-type anionic clays: Preparation, properties and applications. *Catal. Today* **1991**, *11*, 173−301.
(58) Nyambo, C.; Songtipya, P.; Manias, E.; Jimenez-Gasco, M. M.; Wilkie, C. A. Effect of MgAl-layered double hydroxide exchanged with linear alkyl carboxylates on fire-retardancy of PMMA and PS. *J. Mater. Chem.* **2008**, *18*, 4827−4838.
(59) Wang, Y.; Gao, H. Compositional and structural control on anion sorption capability of layered double hydroxides (LDHs). *J. Colloid Interface Sci.* **2006**, *301*, 19−26.
(60) Theiss, F. L.; Ayoko, G. A.; Frost, R. L. Thermogravimetric analysis of selected layered double hydroxides. *J. Therm. Anal. Calorim.* **2013**, *112*, 649−657.
(61) Liu, J.; Song, J.; Xiao, H.; Zhang, L.; Qin, Y.; Liu, D.; Hou, W.; Du, N. Synthesis and thermal properties of ZnAl layered double hydroxide by urea hydrolysis. *Powder Technol.* **2014**, *253*, 41−45.
(62) Grishchenko, R. O.; Emelina, A. L.; Makarov, P. Y. Thermodynamic properties and thermal behavior of Friedel's salt. *Thermochim. Acta* **2013**, *570*, 74−79.
(63) Yao, R.; Wu, X.; Du, Y.; Xie, X.; Wang, Z. Study on the thermal decomposition behavior of MgAl-hydrotalcite compounds. *Adv. Mater. Res.* **2011**, *6*, 152−153.
(64) Zheng, Y. M.; Li, N.; Zhang, W. D. Preparation of nanostructured microspheres of Zn−Mg−Al layered double hydroxides with high adsorption property. *Colloids Surf., A* **2012**, *415*, 195−201.
(65) Magri, V. R.; Duarte, A.; Perotti, G. F.; Constantino, V. R. Investigation of thermal behavior of layered double hydroxides intercalated with carboxymethylcellulose aiming bio-carbon based nanocomposites. *ChemEngineering* **2019**, *3*, 55.

https://doi.org/10.1021/acsomega.2c07395
ACS Omega 2023, 8, 8427−8440

(66) Monteiro, B.; Gago, S.; Paz, F. A. A.; Bilsborrow, R.; Gonçalves, I. S.; Pillinger, M. Investigation of layered double hydroxides intercalated by oxomolybdenum catecholate complexes. *Inorg. Chem.* **2008**, *47*, 8674−8686.
(67) Wang, L.; Lü, Z.; Li, F.; Duan, X. Study on the mechanism and kinetics of the thermal decomposition of Ni/Al layered double hydroxide nitrate. *Ind. Eng. Chem. Res.* **2008**, *47*, 7211−7218.
(68) Guo, L.; Zhang, F.; Lu, J. C.; Zeng, R. C.; Li, S. Q.; Song, L.; Zeng, J. M. A comparison of corrosion inhibition of magnesium aluminum and zinc aluminum vanadate intercalated layered double hydroxides on magnesium alloys. *Front. Mater. Sci.* **2018**, *12*, 198−206.
(69) Yokoi, T.; Tsukada, K.; Terasaka, S.; Kamitakahara, M.; Matsubara, H. Morphological control of layered double hydroxide through a biomimetic approach using carboxylic and sulfonic acids. *J. Asian Ceram. Soc.* **2015**, *3*, 230−233.
(70) Naseem, S.; Gevers, B.; Boldt, R.; Labuschagné, F. J. W.; Leuteritz, A. Comparison of transition metal (Fe, Co, Ni, Cu, and Zn) containing tri-metal layered double hydroxides (LDHs) prepared by urea hydrolysis. *RSC Adv.* **2019**, *9*, 3030−3040.
(71) Bravo-Suárez, J. J.; Páez-Mozo, E. A.; Oyama, S. T. Review of the synthesis of layered double hydroxides: A thermodynamic approach. *Quim. Nova* **2004**, *27*, 601−614.
(72) Prevot, V.; Touati, S.; Mousty, C. Confined growth of NiAl-Layered Double Hydroxide nanoparticles within alginate gel: Influence on electrochemical properties. *Front. Chem.* **2020**, *8*, No. 561975.
(73) Han, Y. U.; Lee, W. S.; Lee, C. G.; Park, S. J.; Kim, K. W.; Kim, S. B. Entrapment of Mg-Al layered double hydroxide in calcium alginate beads for phosphate removal from aqueous solution. *Desalin. Water Treat.* **2011**, *36*, 178−186.
(74) Cardoso, L. P.; Celis, R.; Cornejo, J.; Valim, J. B. Layered double hydroxides as supports for the slow release of acid herbicides. *J. Agric. Food Chem.* **2006**, *54*, 5968−5975.
(75) Silva, V. D.; Mangrich, A. S.; Wypych, F. Nitrate release from layered double hydroxides as potential slow-release fertilizers. *Rev. Bras. Cienc. Solo.* **2014**, *38*, 821−830.
(76) Bi, X.; Zhang, H.; Dou, L. Layered double hydroxide-based nanocarriers for drug delivery. *Pharmaceutics* **2014**, *6*, 298−332.
(77) Borgiallo, A.; Rojas, R. Reactivity and heavy metal removal capacity of calcium alginate beads loaded with Ca−Al layered double hydroxides. *J. Chem. Eng.* **2019**, *3*, 22.
(78) Zhou, H.; Tan, Y.; Gao, W.; Zhang, Y.; Yang, Y. Selective nitrate removal from aqueous solutions by a hydrotalcite-like absorbent FeMgMn-LDH. *Sci. Rep.* **2020**, *10*, No. 16126.
(79) Seida, Y.; Nakano, Y. Removal of phosphate by layered double hydroxides containing iron. *Water Res.* **2002**, *36*, 1306−1312.
(80) Junji, S.; Norihiro, M.; Shinsuke, N. pH buffering action of layered double hydroxide. *Kagaku Kogaku Ronbunshu* **2007**, *33*, 273−277.
(81) Halajnia, A.; Oustan, S.; Najafi, N.; Khataee, A. R.; Lakzian, A. Adsorption−desorption characteristics of nitrate, phosphate and sulfate on Mg−Al layered double hydroxide. *Appl. Clay Sci.* **2013**, *80-81*, 305−312.
(82) Onishi, B. S. D.; dos Reis Ferreira, C. S.; Urbano, A.; Santos, M. J. Modified hydrotalcite for phosphorus slow-release: Kinetic and sorption-desorption processes in clayey and sandy soils from North of Paraná state (Brazil). *Appl. Clay Sci.* **2020**, *197*, No. 105759.
(83) Torres-Dorante, L. O.; Lammel, J.; Kuhlmann, H.; Witzke, T.; Olfs, H. W. Capacity, selectivity, and reversibility for nitrate exchange of a layered double-hydroxide (LDH) mineral in simulated soil solutions and in soil. *J. Plant Nutr. Soil Sci.* **2008**, *171*, 777−784.
(84) Ureña-Amate, M. D.; Boutarbouch, N. D.; del Mar Socias-Viciana, M.; González-Pradas, E. Controlled release of nitrate from hydrotalcite modified formulations. *Appl. Clay Sci.* **2011**, *52*, 368−373.
(85) Berber, M. R.; Hafez, I. H. Synthesis of a new nitrate-fertilizer form with a controlled release behavior via an incorporation technique into a clay material. *Bull. Environ. Contam. Toxicol.* **2018**, *101*, 751−757.
(86) van der Merwe, R. D. T.; Goosen, N. J.; Pott, R. W. M. Macroalgal-derived alginate soil amendments for water retention, nutrient release rate reduction, and soil pH control. *Gels* **2022**, *8*, 548.
(87) Oladosu, Y.; Rafii, M. Y.; Arolu, F.; Chukwu, S. C.; Salisu, M. A.; Fagbohun, I. K.; Muftaudeen, T. K.; Swaray, S.; Haliru, B. S. Superabsorbent polymer hydrogels for sustainable agriculture: A review. *Horticulturae* **2022**, *8*, 605.
(88) Taha, T. H.; Elnouby, M. S.; Abu-Saied, M. A.; Alamri, S. Tested functionalization of alginate-immobilized ureolytic bacteria for improvement of soil biocementation and maximizing water retention. *RSC Adv.* **2020**, *10*, 21350−21359.
(89) Liu, S.; Wu, Q.; Sun, X.; Yue, Y.; Tubana, B.; Yang, R.; Cheng, H. N. Novel alginate-cellulose nanofiber-poly (vinyl alcohol) hydrogels for carrying and delivering nitrogen, phosphorus and potassium chemicals. *Int. J. Biol. Macromol.* **2021**, *172*, 330−340.
(90) Liu, G.; Hanlon, E. Soil pH range for optimum commercial vegetable production *EDIS* 2012, *2012*, Corpus ID: 37866956 DOI: 10.32473/edis-hs1207-2012.

https://doi.org/10.1021/acsomega.2c07395
ACS Omega 2023, 8, 8427−8440